NGI Technical note

To:	Norges vassdrags- og energidirektorat (NVE)
Attn.:	Odd Are Jensen
Copy to:	CJ, KGi, PG, HHH
Date:	2023-08-24
Revision no./Rev.date:	0/
Document no.:	20200017-03-TN
Project:	Applied Avalanche Research in Norway (AARN)
Project manager:	Kjersti G. Gisnås
Prepared by:	Dieter Issler
Reviewed by:	Elise Morken

A Simple Model for the Variability of Release Area Size

Abstract

The hazard mapping tool NAKSIN estimates the release probability of potential release areas (PRAs) by testing a stability criterion based on the infinite-slope approximation with a large sample of synthetic weather situations. The release area is thus assumed to comprise the entire PRA, which is unrealistic for avalanches with return periods shorter than 100–300 y. To remedy this, a stability criterion is proposed that accounts for stabilizing forces across the slab perimeter and so is sensitive to the slab extent. The criterion is applied to a sequence of subareas of the PRA with increasing minimum slope angle to find the subarea with maximum release probability. The method is described and formulated mathematically. Also, tools for coding it are suggested but implementation in NAKSIN and testing are left for future work.

Contents

NORWEGIAN GEOTECHNICAL INSTITUTE
NGI.NO

Main office
PO Box 3930 Ullevaal St.
NO-0806 Oslo
Norway

Trondheim office
PO Box 5687 Torgarden
NO-7485 Trondheim
Norway

T 22 02 30 00
F 22 23 04 48
NGI@ngi.no

BIC NO. DNBANOKK
IBAN NO26 5096 05 01281
ORGANISATION NO.
958 254 318MVA

ISO 9001/14001
CERTIFIED BY BSI
FS 32989/EMS 612006

1 Introduction

Since 2015, NGI has been developing Nye AktsomhetsKart for Snøskred i Norge (NAKSIN), a tool for creating detailed and high-quality avalanche susceptibility maps (more precisely, avalanche hazard indication maps) in a largely automated way (Issler *et al.*, 2023). First, NAKSIN determines all potential release areas (PRAs) in the study area using topographic criteria. For each of these PRAs, the release probability is estimated, and if it exceeds a threshold set by the user, the fracture depth d_0 associated with the threshold probability is calculated. With a slab of thickness d_0 covering the entire PRA as initial condition, the run-out of this avalanche is simulated with the quasi-3D dynamical model MoT-Voellmy. The final hazard indication map is the union of all grid cells hit by one or more avalanches.

Perhaps the most innovative aspect of NAKSIN is the calculation of release probability for each PRA, following an approach outlined by Gauer (2018):

1. Time series of daily weather data (mean air temperature, precipitation, snow height and snow water equivalent, new snow height and new-snow water equivalent) from SeNorge are interpolated (or extrapolated) from the nearest 1 km^2 SeNorge grid cells to the PRA in question.

2. Probability distribution functions (PDFs) are directly derived from the weather data and used to infer the mean values of relevant snow parameters like density and shear strength of an assumed weak layer somewhere in the old-snow cover.

3. With these PDFs, augmented by PDFs for the location of the weak layer and the distribution of the weak-layer shear strength around its average, a large set (typically 1–5 millions) of synthetic snowfall situations are generated for each PRA.

4. For each PRA, the annual probability of avalanche release is computed by evaluating the balance of driving and resistive forces in the infinite-slope approximation for all synthetic “snowfalls” and counting the number of unstable situations. In this approximation, gravity as the driving force is resisted by the shear strength of the weak layer.

5. For the samples that lead to avalanche release, the fracture depth of an event with a user-defined target return period is determined from the distribution of simulated fracture depths.

An important shortcoming of this scheme is its assumption that the release area always comprises the entire PRA, independent of the return period of the event. It is well known that this is a valid approximation only for avalanche events with very long return periods—typically above 100–300 y (Maggioni & Gruber, 2003; Maggioni *et al.*, 2006). The length and often also the width of the run-out area increase with the size of the release area, with all other parameters held constant. Moreover, the calibration used for the friction parameters (Bartelt *et al.*, 2017) depends on the release volume, so

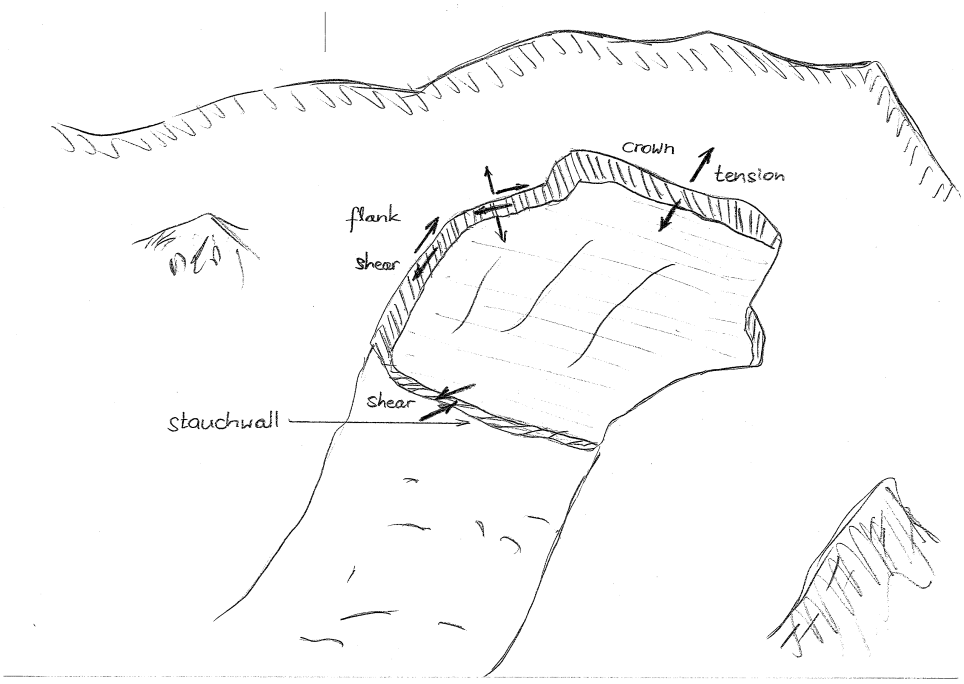

Figure 1 Schematic drawing of the release area of a slab avalanche. The slab is supported by the shear strength τ of the weak layer, the compressive strength σ_c acting across the stauchwall, the tensile strength σ_t across the crown, and the shear strength σ_s along the sidewalls of the fracture line.

overestimating the release area may lead to overestimating the run-out area. However, at present there is no established method for determining the dependence of the release area on the return period of an avalanche event.

The objective in this Technical Note is therefore to find a physically reasonable yet practically applicable method for achieving this. This is equivalent to finding the cumulative probability distribution function (CPDF) of release area, $P(A)$, which is the conditional probability for the release area to be at least A if there is an avalanche release. It is desirable that this method be compatible with the general approach used in NAKSIN so that it can be implemented there without massive changes to the structure of the code.

2 Derivation of the method

Summary of the approach The proposed method rests on a few simple observations:

1. In the infinite-slope approximation, the factor of safety, $I_{S,\infty}(\psi)$, of a slab with given height h (measured vertically) and weak-layer shear strength τ is infinite for horizontal ($\psi = 0°$) and vertical ($\psi = 90°$) slopes, and it has a minimum at $\psi = 45°$, see Eqs. (1) and (2) below.

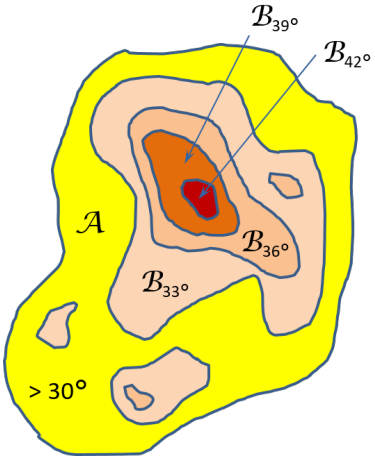

Figure 2 Patches $\mathcal{B}_\theta$ of increasing minimum slope angle θ and decreasing size $A(\theta)$ within a potential release area $\mathcal{A}$ (yellow).

2. The factor of safety of a finite-size slab of depth h, perimeter length L and area A on an inclined plane with slope angle θ is larger than for an infinite slab, $I_S(\theta, A, h) > I_{S,\infty}(\theta, h)$, because of the stabilizing forces acting along the perimeter of the slab, characterized by the mean strength σ, as shown in Fig. 1 (Lackinger, 1989).

3. Both the driving force of gravity and the stabilizing force due to the shear strength of the weak layer are proportional to the slab area, whereas the stabilizing forces along the slab perimeter are proportional to the perimeter length and an average value σ of tensile, compressive and shear strength in the slab (Fig. 1).

4. In a real avalanche release area, the slope angle varies spatially. The largest connected area for which the slope angle exceeds some value θ, $\tilde{A}(\theta)$, is a monotonically decreasing (but not necessarily continuous[1]) function of θ. There is a corresponding function $\tilde{L}(\theta)$ for the length of the perimeter, but its decrease need not be monotonic.

Consider a PRA $\mathcal{A}$ with area $A_\mathcal{A}$ and perimeter $L_\mathcal{A}$; denote its minimum, maximum and average slope angles by θ_{low}, θ_{high} and $\psi_\mathcal{A}$, respectively. Let $\tilde{L}(\theta)$ and $\tilde{A}(\theta)$ be the perimeter and area of the largest *connected* patch in $\mathcal{A}$—termed $\mathcal{B}_\theta$—inside which the local slope angle is at least θ (Figs. 2 and 3). The *average* slope angle of the patches $\mathcal{B}_\theta$, $\psi(\theta)$ need not always increase monotonically with θ, but $\theta_{\min} \le \theta \le \psi(\theta) \le \theta_{\max}$, see Fig. 3. Clearly, $\tilde{A}(\theta_{\min}) = A_\mathcal{A}$ and $\tilde{L}(\theta_{\min}) = L_\mathcal{A}$. Moreover, in typical terrain $\tilde{A}(\theta) \to 0$ and $\tilde{L}(\theta) \to 0$ as $\theta \to \theta_{\text{high}}$, which we will assume to hold[2]. $\tilde{A}(\theta)$ decreases monotonically with increasing θ, but this is not generally true for $\tilde{L}(\theta)$.

[1]Consider a patch $\mathcal{B}_0$ consisting of three subpatches $\mathcal{B}_1$, $\mathcal{B}_2$, $\mathcal{B}_3$ with slope angles $\theta_1 < \theta_2 < \theta_3$ and assume that $\mathcal{B}_2$ and $\mathcal{B}_3$ do not touch each other. Then $A(\theta) = A_1 + A_2 + A_3$ for $\theta \le \theta_1$. For $\theta_1 < \theta \le \theta_2$, one has $A(\theta) = A_2 + A_3$, and for $\theta_2 < \theta \le \theta_3$, $A = A_3$.

[2]It is, however, not difficult to construct a counter-example: Imagine a mountain slope consisting of a

Next, assume that there is a weak snow layer covering the slope including $\mathcal{A}$ and that new snow is falling indefinitely. For each new-snow height h, among the innumerable patches $\mathcal{B}_\theta$ in $\mathcal{A}$ there is one patch $\mathcal{B}_{\theta_*(h)}$ for which the factor of safety is lowest, i.e., $I_S(\mathcal{B}_{\theta_*(h)}, h) = \min(I_S(\mathcal{B}_\theta, h))$ for all $\theta \in [\theta_{\text{low}}, \theta_{\text{high}}]$, and $\theta_*(h)$ is lowest if there is more than one slope angle θ' for which $I_S(\mathcal{B}_{\theta'}, h) = \min(I_S(\mathcal{B}_\theta, h))$.

We further assume that the snow cover is not unconditionally stable. Such would be the case if the stabilizing forces transmitted across the perimeter of the patch all by themselves exceeded the down-slope gravitational force on the slab, $\sigma\tilde{L}(\theta) > \rho\tilde{A}(\theta)g\sin\theta$, for all $\theta \in [\theta_{\text{low}}, \theta_{\text{high}}]$. ρ is the density of the new snow forming the slab. Under such conditions, the factor of safety decreases as the snow accumulates, but its asymptotic value is larger than 1. Conversely, if $\sigma\tilde{L}(\theta) < \rho\tilde{A}(\theta)g\sin\theta$ for some range of θ, the minimum factor of safety will eventually become 1—the critical condition for avalanche release in this simplified model—for some new-snow height $h = h_r$ (measured verically) and release angle $\theta_*(h_r)$. The corresponding patch area $\tilde{A}(\theta_*(h_r))$ is the sought release area. An avalanche releases from that patch if and as soon as the snowfall height attains the value h_r. The corresponding fracture *depth* is approximated as $d_f \approx h_r \cos\psi(\theta_*)$, where $\psi(\theta_*)$ is the average slope angle of the patch $\mathcal{B}_{\theta_*(h_r)}$.

θ_* depends on ρ, σ and τ. In the mathematical formulation of this mechanism, we will provisionally assume that the angle $\theta_*(h)$ is unique and that $\tilde{A}(\theta)$ and $\tilde{L}(\theta)$ are differentiable and monotonically decreasing with increasing θ, even though both functions have discontinuities in reality and $\tilde{L}(\theta)$ also may have local maxima. The strength σ is the average of the tensile, compressive and shear strength of the slab, weighted with the relative lengths of the crown, the stauchwall and the flanks. For simplicity, we also assume that this weighting is independent of θ (and h). In reality, σ depends on the shape of the patch and may change with θ.

Size-dependence of the factor of safety We start by assuming that the mean slope angle of patches, $\psi_{\mathcal{B}(\theta)}$, is a *monotonic* function of the minimum angle, θ, associated with the patch, see Fig. 3. This ensures that the relation between ψ and θ is invertible (numerically). Then, we may define new functions A and L through the relations $A(\psi(\theta)) := \tilde{A}(\theta)$ and $L(\psi(\theta)) := \tilde{L}(\theta)$.

In the infinite-slope approximation, the factor of safety on a slope of uniform inclination ψ is

$$I_{S,\infty}(\psi, h) = \frac{\tau}{\rho g h \cos\psi \sin\psi} = \frac{2\hat{\tau}}{h\sin(2\psi)}, \tag{1}$$

where τ is the shear strength of the weak layer and $\hat{\tau} := \tau/(\rho g)$ has the dimension of a length. For $\psi \to 0°$ and $\psi \to 90°$, $I_{S,\infty}$ tends to ∞, and it attains its minimum value $2\hat{\tau}/h$ at $\psi = 45°$. In the present context, it is advantageous to work with a force residue

gently inclined plane with $\theta = \theta_{\text{low}}$ in its lower part and a steep inclined plane with $\theta = \theta_{\text{high}}$ in its upper part.

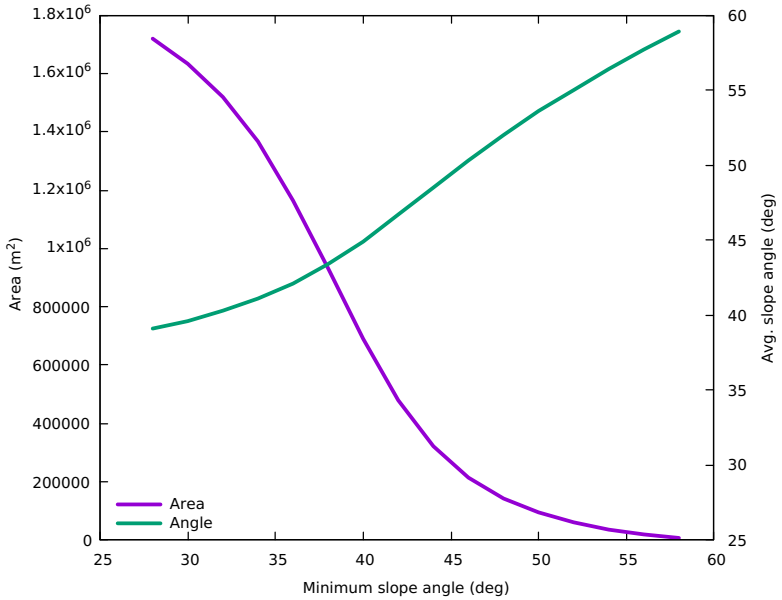

Figure 3 Example of how the total *area* $\sum_l A_l(\theta)$ *that is steeper than a minimum angle* θ *decreases with* θ *(lilac curve, left-hand axis) and how the* average *slope angle* ψ *of this total area increases with* θ *(green curve, right-hand axis). The area* $A_1(\theta)$ *of the* largest *patch steeper than* θ *decreases much more rapidly with* θ *than* $\sum_l A_l(\theta)$*. Data drawn from the Midaou avalanche path in the French Pyrenees.*

function instead:

$$R_\infty(\psi, h) := \hat{\tau} - h \sin\psi \cos\psi, \tag{2}$$

where $R_\infty < 0$ implies instability.

If one includes the peripheral forces on a snow slab of area A and perimeter L corresponding to a connected patch $\mathcal{B}$, the force residue becomes

$$\begin{aligned} R(\psi, h) &= \hat{\tau}A(\psi) + \hat{\sigma}L(\psi)h\cos\psi - A(\psi)h\cos\psi\sin\psi \\ &= A(\psi)(\hat{\tau} - h\cos\psi\sin\psi) + \hat{\sigma}L(\psi)h\cos\psi \\ &= A(\psi)[\hat{\tau} - h(\sin\psi - \hat{\sigma}\Lambda(\psi))\cos\psi]. \end{aligned} \tag{3}$$

Here, we have defined $\Lambda(\psi) := L(\psi)/A(\psi)$ with units of inverse length and the scaled slab strength $\hat{\sigma} := \sigma/(\rho g)$, which characterizes the slab properties and has units of length. $\hat{\sigma}$ is typically an order-of-magnitude larger than $\hat{\tau}$ because (i) the shear strength of the weak layer is usually much lower than that of the overlying slab and (ii) the compressive strength, which is substantially larger than the shear strength, contributes to σ.

Equation (3) is, strictly speaking, only valid for a slab on an inclined plane. To apply it to a slab on curved terrain, the numerator should be extended to vectorial form and expressed as surface integrals while the denominator is to be evaluated as a volume integral. For

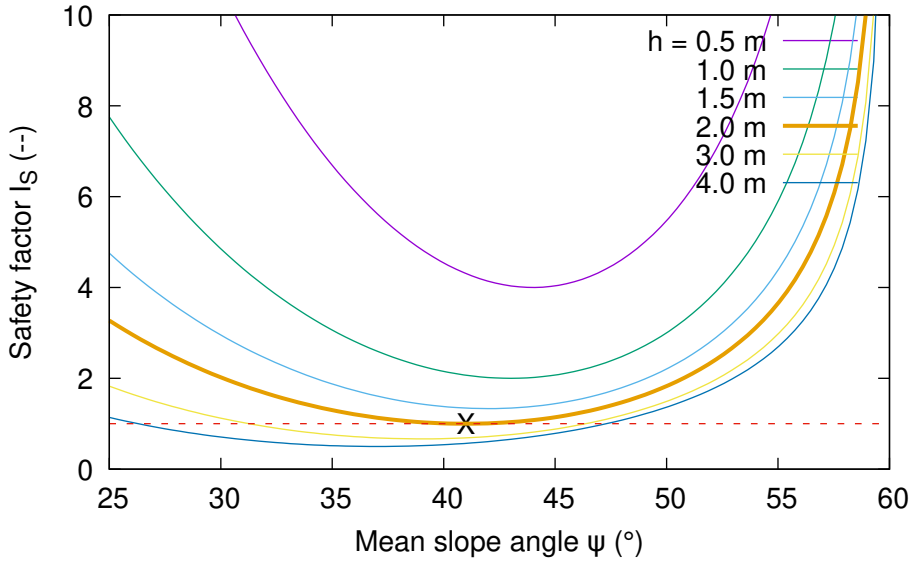

Figure 4 Qualitative dependence of the factor of safety, I_S, on the mean slope angle ψ for different values of the new-snow height h. The thick curve touching the line $I_S = 1$ represents the fracture height for this synthetic event, the abscissa of the marked point indicates the mean slope angle of the release patch within the PRA.

the sake of simplicity, we here work with the average slope angle in $\mathcal{B}_\theta$:

$$\psi(\theta) := \int_{\mathcal{B}_\theta} \phi(x) \mathrm{d}A. \tag{4}$$

For given $\hat{\tau}$ and $\hat{\sigma}$, the force residue is a function of the two variables ψ and h. The qualitative behavior of the closely related factor of safety, I_S, is illustrated in Fig. 4 for six values of h and assuming that the local slope angles within the PRA range from $\theta_{\text{low}} = 30^\circ$ to $\theta_{\text{high}} = 60^\circ$. Note that the plot is not based on actual data, but with the stated assumptions the curves must diverge as $\psi \to 60^\circ$ and $\psi \to 0^\circ$.

During a snowfall, as h increases steadily, the stability of the slope is characterized by progressively lower-lying curves in Fig. 4 and described by the function $R(\psi, h(t))$ at time t. The avalanche will be released when the minimum of this function crosses the horizontal line $R = 0$ (or $I_S = 1$ in Fig. 4). The parameter $h = h_r$ of the curve that touches the line $R = 0$ (or $I_S = 1$) is the (vertically measured) fracture height, and the abscissa $\psi = \psi_r$ of the tangent point is the mean slope angle of the release patch. From ψ_r, θ_r, the release area $A(\psi_r)$ and domain $\mathcal{B}_{\theta(\psi_r)}$ for this event follow immediately.

If we furthermore assume that $R(\psi, h)$ is differentiable and, for any fixed value of h, only has a single minimum, the release condition for a finite slab can be formulated as

$$R(\psi_r, h_r) = 0 \qquad \text{and} \qquad \frac{\partial R}{\partial \psi}(\psi, h)\bigg|_{\psi_r, h_r} = 0. \tag{5}$$

From Eq. (3), the first of the conditions (5) can readily be solved for h_r in terms of ψ:

$$h_r(\psi) = \frac{\hat{\tau}}{[\sin\psi - \hat{\sigma}\Lambda(\psi)]\cos\psi}. \tag{6}$$

To find the patch $\mathcal{B}_{\theta(\psi_r)}$ that is the first to become unstable during the snowfall, i.e., with the minimum value of h, one uses the second condition in Eq. (5). This is a condition for the partial derivative of I_S with respect to ψ, i.e., h is to be kept fixed. Only after taking the derivative is one to substitute the expression (6) for h_r as a function of ψ:

$$\begin{aligned}\frac{\partial R}{\partial \psi} = {} & A'(\psi)\,[\hat{\tau} - h(\sin\psi - \hat{\sigma}\Lambda(\psi))\cos\psi] \\ & + A(\psi)h\left[\hat{\sigma}[\Lambda'(\psi)\cos\psi - \Lambda(\psi)\sin\psi] - \cos(2\psi)\right],\end{aligned}$$

which simplifies immediately because the factor multiplying $A'(\psi)$ vanishes at $h = h_r$ according to the first condition in Eq. (5). Thus one obtains

$$Q(\psi_r) := \hat{\sigma}[\Lambda'(\psi_r)\cos\psi_r - \Lambda(\psi_r)\sin\psi_r] - \cos(2\psi_r) = 0. \tag{7}$$

Once ψ_r has been determined, h_r follows from Eq. (6).

Qualitative behavior Without an explicit form of the function $\Lambda(\psi)$, the highly non-linear Eq. (5) cannot be solved. Since $\Lambda(\psi)$ is not known in analytic form for a natural terrain, numerical techniques must be used. However, a few statements about the existence and properties of solutions can be made.

First—perhaps surprisingly—the shear strength of the weak layer, τ, does not appear in Eq. (7). This comes about because both the driving gravitational force and the supporting forces across the periphery of the slab are proportional to the slab height, h, whereas the supporting force from the shear strength of the weak layer is independent of h and of ψ. Thus, $\hat{\sigma}$ determines the critical angle for release while the fracture height depends linearly on $\hat{\tau}$.

Second, one should generally expect discontinuities to occur in $A(\psi)$ and $L(\psi)$, as Fig. 2 illustrates: In that example, the patch $\mathcal{B}_{30^\circ}$ splits into a large one and two small ones as θ is increased from 30° to 33°, and similarly between 33° and 36°. Where this occurs, A, L and Λ have discontinuities. An implementation of this model must therefore search for solutions of Eq. (7) in each interval where $\Lambda(\psi)$ is continuous.

Third, as ψ approaches θ_{high} from below, $A(\psi) \to 0$ and $L(\psi) \to 0$ in normal terrain so that Λ increases as $A^{-1/2}$ and R thus vanishes as $A^{1/2}$. If $R(\theta_{\text{high}}) = 0$ and $A(\theta_{\text{high}} - \epsilon) \propto \epsilon^a$ for small values of ϵ, R has a horizontal tangent at θ_{high} for $a > 1$. However, this solution is practically irrelevant because the release area would be 0. One exception from this behavior is described in Footnote 2, with A, L and Λ taking finite values and an avalanche releasing as soon as the new-snow height attains the value $h_r(\theta_{\text{high}})$. (Another

theoretical possibility is the patch showing fractal behavior, with A tending to 0 but L remaining finite; R could then approach a finite positive limit.)

Fourth, if one expresses Eq. (3) in terms of the factor of safety,

$$I_S(\psi, h) := \frac{\hat{\tau} + \hat{\sigma}\Lambda(\psi)h\cos\psi}{h\sin\psi\cos\psi}, \tag{8}$$

one sees that $I_S(\psi, h)|_{\psi=\text{cst.}}$ decreases with increasing h and tends to the limit

$$I_S^{\min}(\psi) = \lim_{h\to\infty} I_S(\psi, h) = \hat{\sigma}\,\frac{\Lambda(\psi)}{\sin\psi}. \tag{9}$$

Depending on the values of $\hat{\sigma}$, Λ and ψ, this may be smaller or larger than 1. If $I_S^{\min} > 1$, the patch is unconditionally stable. This is in marked contrast to the infinite-slope approximation where instability is inevitable if only h is large enough. The reason is that not only the gravitational force but also the stabilizing forces across the perimeter of the slab grow linearly with h.

Fifth, in the infinite-slope approximation (1), $I_{S,\infty}(45^\circ+\alpha, h) = I_{S,\infty}(45^\circ-\alpha, h)$ for any angle α, i.e., there is symmetry about $\psi = 45^\circ$. Equation (8) shows how the contribution from the perimeter forces breaks this symmetry. ψ_r is pushed below 45° if $\Lambda'(45^\circ) < \Lambda(45^\circ)$, and above 45° otherwise. (Note that, when taking the derivative of Λ, dψ is to be measured in radians.) However, without further information on the function $\Lambda(\psi)$, such questions cannot be answered definitively.

3 Pointers towards implementation in NAKSIN

Determination of the functions $L(\psi)$ and $A(\psi)$ Given a digital terrain model comprising the PRA, $L(\psi)$ and $A(\psi)$ can be obtained for a set $\{\theta_i\}$ of lower thresholds and a corresponding set $\{\psi_i\}$ of mean slope angles, $\psi_1 < \psi_2 < ... < \psi_n$ with $\theta_{\text{low}} < \psi_1 < ... < \psi_n \leq \theta_{\text{high}}$ using functions provided in a geographical information system (GIS) or packages like GDAL/OGR. The obtained values are tabulated, and the $\{\psi_i\}$ should be spaced densely enough to allow meaningful interpolation—this is particularly important for estimating the derivative of $\Lambda(\psi)$.

With a view towards implementation in NAKSIN, which needs to estimate the total annual release probability in a given PRA, one scenario neglected so far must be considered: Using Fig. 2 as an example, suppose that the patch $\mathcal{B}_{39^\circ}$ is most prone release in a given situation. In a severe snow storm, an avalanche may release from it early during the storm. But as the snow continues falling, one or both of the disjoint patches with minimum slope angle 36° might also become unstable and produce avalanches. These events ought to be counted as well and their fracture heights and patches recorded. This will matter for the total release probability and for the release volume of the "target" avalanche, for which NAKSIN will calculate the run-out. Moreover, in APALI, an extension

of NAKSIN for probabilistic hazard mapping (Issler, 2023), probability distribution functions of the release area and the fracture height must be extracted from the Monte Carlo simulation results, which must include these minor releases as well.

This circumstance requires a data structure that can track the branching of a PRA in several smaller partial release areas with increasing θ_i. This structure must allow to determine, for any patch $\mathcal{B}_j$ prone to release when the new-snow depth reaches the threshold h_j, whether it is part of, or contains, another patch $\mathcal{B}_k$ with lower threshold $h_k < h_j$. One may then exclude $\mathcal{B}_j$ from releasing or increase its threshold h_j. This requirement suggests that each patch be given a unique identifier and carry a list containing the identifiers of its "parent" patches.

The analysis proceeds through the following steps:

1. Calculate the local slope angle θ for each DTM cell inside the PRA.
2. For sufficiently many values θ_i, find the sets $\mathcal{U}_i$ with $\theta \geq \theta_i$ for all cells in $\mathcal{U}_i$.
3. In each $\mathcal{U}_i$, find and store the connected subsets $\mathcal{B}_{i,k}$, their mean slope angles $\psi_{i,k}$, areas $A_{i,k}$ and perimeters $L_{i,k}$.
4. Reconstruct the "genealogic tree" (GT) of each PRA, starting from the "twigs", i.e., the patches that do not contain further subpatches of the "tree of patches". For each twig, there is a genealogic line going back to the PRA $\mathcal{A}$, which gives rise to an array $\mathcal{L}_g = \{\Lambda(\psi_{i,k})\}$ associated with the patches $\{\mathcal{B}_{i,k}\}$.
5. For the given values of $\hat{\tau}$ and $\hat{\sigma}$ and for each genealogic line, find the critical slope angle ψ_r and the corresponding fracture height h_r from Eq. (7), using $\Lambda(\psi)$ interpolated from its array $\mathcal{L}_g$. Record all these data in a sorted list of release events, which will be used later in the NAKSIN workflow.

If one uses Python for this analysis, the functions `scipy.ndimage.generate_binary_structure`, `scipy.ndimage.label` and `numpy.unique` will be handy. To obtain the perimeter of a connected patch, it may be best to first vectorize the patch and then use analysis tools for vector data to get the perimeter. The first step can be accomplished with, e.g., the `gdal.polygonize` function from the GDAL library. For calculating the perimeter of the polygon, the class `Polygon` from the Python module `shapely.geometry` has an attribute `.length` that can be used for the purpose.

Solution of the stability equation for ψ To solve Eq. (7) for ψ_r, one calculates the value of $Q(\psi_i)$ for the set of mean slope angles ψ_i derived from the patches $\mathcal{B}_{\theta_i}$. If the ψ_i are spaced closely enough, a linear interpolation between the values ψ_j with $Q(\psi_j) > 0$ and ψ_{j+1} with $Q(\psi_{j+1}) < 0$ may suffice.

After ψ_r has been found, h_r follows directly from substituting the value of ψ_r in Eq. (6). Finally, A_r is obtained by interpolation of the tabulated values $A(\psi_i)$. If the ψ_i are sufficiently densely spaced, the patch $\mathcal{A}_r(\psi_j)$, where ψ_j is the tabulated value nearest to ψ_r, will give an adequate approximation of the release area.

Required modifications of the NAKSIN program structure The modular structure of NAKSIN restricts the necessary changes to the modules `release_area.py`, which so far only determines the PRAs, and `release_prob.py`, where the release probability and fracture depth are calculated for a large number of synthetic weather and snow situations.

Like the original version, the modified version of `release_area.py` carries out all topographical operations: finding the maximal PRAs and applying the same constraints on terrain curvature and connectedness as before. It may no longer be necessary to restrict the vertical or areal extent of PRAs because very small areas tend to be eliminated by the stabilizing effect of the surrounding snow cover and very large or long areas tend to be divided into subpatches that have higher release probability than the full PRA.

In addition, the subpatches have to be identified and quantified as described above, and a data structure describing the GT of each PRA created. As in the present version, the module outputs one or two large lists (with or without forest effects included, `patches_wf` and/or `patches_nf`). In contrast to earlier with entries for each PRA, these lists contain entries for each node in the GT. Each entry in these lists is itself a list collecting all relevant information on the patch, with two new elements, namely its associated value of Λ and its GT (which is a list itself). Furthermore, for each patch, a raster or vector file defining the patch must be stored for potential use in the run-out calculations.

In the module `release_prob.py`, the main changes are the following:

- Besides the scaled weak-layer shear strength $\hat{\tau}$, the scaled average slab strength $\hat{\sigma}$ must be estimated.
- The release criterion is changed to implement Eq. (5).
- For each synthetic “snow storm”, the stability must be evaluated not only for the PRA but also for all nodes on its GT.
- If there is a release in a patch during a “storm”, the release conditions (particularly the available snow height) must be adjusted for all patches that are affected by it.
- All registered releases in a GT must be consolidated into one sorted list to determine the annual release probability of the corresponding PRA and the fracture height and associated release patch for a given target return period.

4 Outlook

The proposed method first needs critical scrutiny. If no major flaws are found, it needs to be tested thoroughly. This can be done either with custom-made scripts used in case studies or by implementing it in NAKSIN as sketched in the preceding section.

The precise way in which the effect of an avalanche release in one patch affects the release probability in other patches in the same GT must be investigated in more detail. In Nature, it is often observed that more than one avalanche releases from a PRA in the course of one storm. Sometimes, the avalanches release from disjoint patches with different snow properties or loading conditions. It may, however, also happen that the same patch is involved in a subsequent release because blowing snow has recharged the snow cover in the patch area. There are several possible ways to incorporate this in the model; in view of the large areas to be mapped by NAKSIN, a good compromise between completeness of the model and computational performance must be found.

The possibility of avalanches releasing from two separate patches in the same PRA (or even in different PRAs threatening the same run-out area) highlights a general problem in hazard mapping, which is often either neglected or only addressed through expert judgment: Consider two avalanche paths, each with annual release probability $0.0007\,\mathrm{a}^{-1}$, which would not lead to building restrictions for familiy homes in Norway. However, where their run-out areas intersect, the annual probability exceeds $0.0014\,\mathrm{a}^{-1}$ and thus the regulated threshold for construction permits. This problem is not satisfactorily handled in the present version of NAKSIN, and including variable release-area size may accentuate the problem. Solving it in a satisfactory way is not straightforward unless one adopts a fully probabilistic framework, which requires a much larger computational effort.

This report has not addressed the question how forest effects should be included in the scheme, particularly if the stand density depends significantly on the slope angle. One may average the relevant parameters like stand density, crown coverage and tree diameter separately for each patch. It is, however, not clear yet how best to treat large spatial variability of these parameters within a PRA or a patch.

One may expect that accounting for the dependence of release-area extent on the return period will lead to two opposite effects:

- In areas with high avalanche release probability due to high precipitation, one may expect significantly smaller potential hazard areas if the return period is chosen as 30 or 100 y rather than the 1000 y applied in the new, third-generation avalanche hazard indication maps (AHIM). Judging from exploratory simulations with NAKSIN 3 and 4, which always use the entire PRA, for return periods of 100 years or less, there is strong reason to believe that this effect would make an AHIM targeted at buildings in security class S1 more realistic.
- In areas where the avalanche release probability is generally low and where the mountain sides mostly are not steeper than 30–35° but contain significantly steeper subareas, small to medium-size avalanches may have considerably higher release probability than the entire PRA.

Further effects will likely appear when the model is being tested extensively. One will also want to compare the model and the release areas it predicts with different approaches,

which emphasize topographic features like slope breaks, differences in aspect, and terrain roughness but do not include explicit mechanical stability evaluation as NAKSIN does (Bühler *et al.*, 2013; Veitinger *et al.*, 2016). Most likely, combining different approaches could improve the accuracy of the model, but it remains to see how this can be implemented in a future model that can assess avalanche hazard at the scale of entire countries.

Acknowledgements

The R&D work leading to this paper was carried out within the project Applied Avalanche Research in Norway (AARN), which is financed by the Norwegian Department of Petroleum and Energy (OED) through a special grant for avalanche research at NGI, administrated by the Norwegian Water Resources and Energy Directorate (NVE). The author thanks his colleagues in the AARN project for useful discussions and Elise Morken and Sparsha Sinduri Nagula for critical reading of the manuscript.

References

Bartelt, P., Bühler, Y., Christen, M., Deubelbeiss, Y., Salz, M. *et al.* (2017). *RAMMS::AVALANCHE User Manual*. URL https://ramms.slf.ch/fileadmin/user_upload/WSL/Microsite/RAMMS/Downloads/RAMMS_AVAL_Manual.pdf. Version 1.7.0.

Bühler, Y., Kumar, S., Veitinger, J., Christen, M., Stoffel, A. *et al.* (2013). Automated identification of potential snow avalanche release areas based on digital elevation models. *Natural Haz. Earth Syst. Sci.* **13**, 1321–1335. doi:10.5194/nhess-13-1321-2013.

Gauer, P. (2018). Avalanche probability: slab release and the effect of forest cover. *In: Proceedings of the Intl. Snow Science Workshop Innsbruck 2018*, pp. 76–83. International Snow Science Workshop. URL http://arc.lib.montana.edu/snow-science/objects/ISSW2018_P01.13.pdf.

Issler, D. (2023). APALI – Avalanche Probability Along Linear Infrastructure. NGI Technical Note 20200431-01-TN, Norwegian Geotechnical Institute, Oslo, Norway.

Issler, D., Gisnås, K. G., Gauer, P., Glimsdal, S., Domaas, U. *et al.* (2023). NAKSIN -– a New Approach to Snow Avalanche Hazard Indication Mapping in Norway. doi:10.2139/ssrn.4530311. URL https://ssrn.com/abstract=4530311. Submitted for publication.

Lackinger, B. (1989). Supporting forces and stability of snow-slab avalanches: a parameter study. *Annals Glaciol.* **13**, 140–145. doi:10.1017/s0260305500007783.

Maggioni, M. & Gruber, U. (2003). The influence of topographic parameters on avalanche release dimension and frequency. *Cold Regions Sci. Technol.* **37**, 407–419. doi:10.1016/S0165-232X(03)00080-6.

Maggioni, M., Gruber, U., Purves, R. S. & Freppaz, M. (2006). Potential release areas and return period of avalanches: Is there a relation? *In: Proceedings of the 2006 International Snow Science Workshop, Telluride, Colorado*, pp. 566–571. URL http://arc.lib.montana.edu/snow-science/item/981.

Veitinger, J., Purves, R. S. & Sovilla, B. (2016). Potential slab avalanche release area identification from estimated winter terrain: a multi-scale, fuzzy logic approach. *Natural Haz. Earth Syst. Sci.* **16**(10), 2211–2225. doi:10.5194/nhess-16-2211-2016.

Kontroll- og referanseside / Review and reference page

Dokumentinformasjon/*Document information*		
Dokumenttittel/*Document title* A Simple Model for the Variability of Release Area Size		**Dokumentnr./*Document no.*** 20200017-03-TN
Dokumenttype/*Type of document* Teknisk notat / *Technical note*	**Oppdragsgiver/*Client*** Norges vassdrags- og energidirektorat (NVE)	**Dato/*Date*** 2023-08-24
Rettigheter til dokumentet iht kontrakt/*Proprietary rights to the document according to contract* ÅPEN: Skal tilgjengeliggjøres i åpent arkiv (BRAGE) / *OPEN: To be published in open archives (BRAGE)*		**Rev.nr. & dato/*Rev.no. & date*** 0 /
Distribusjon/Distribution		
Emneord/*Keywords* Snow avalanches, avalanche release, slope stability, release probability, release area size, NAKSIN		

Stedfesting/*Geographical information*	
Land, fylke/*Country* —	**Havområde/*Offshore area*** —
Kommune/*Municipality* —	**Feltnavn/*Field name*** —
Sted/*Location* —	**Sted/*Location*** —
Kartblad/*Map* —	**Felt, blokknr./*Field, Block No.*** —
UTM-koordinater/*UTM coordinates* **Sone:** — **Øst:** — **Nord:** —	**Koordinater/*Coordinates*** **Projeksjon, datum:** — **Øst:** — **Nord:** —

Dokumentkontroll/*Document control*
Kvalitetssikring i henhold til/*Quality assurance according to* NS-EN ISO9001

Rev.	**Revisjonsgrunnlag/*Reason for revision***	**Egenkontroll av/*Self review by:***	**Sidemanns-kontroll av/ *Colleague review by:***	**Uavhengig kontroll av/ *Independent review by:***	**Tverrfaglig kontroll av/ *Interdisciplinary review by:***
0	Originaldokument	Dieter Issler 2023-08-12	Elise Morken 2023-08-01		Sparsha S. Nagula 2023-08-02

Dokument godkjent for utsendelse / *Document approved for release*	**Dato/*Date***	**Prosjektleder/*Project Manager***
	2023-08-24	Kjersti G. Gisnås

NGI (Norwegian Geotechnical Institute) is a leading international centre for research and consulting within the geosciences. NGI develops optimum solutions for society and offers expertise on the behaviour of soil, rock and snow and their interaction with the natural and built environment.

NGI works within the following sectors: Offshore energy – Building, Construction and Transportation – Natural Hazards – Environmental Engineering.

NGI is a private foundation with office and laboratory in Oslo, branch office in Trondheim and daughter companies in Houston, Texas, USA and in Perth, Western Australia.

www.ngi.no

NGI (Norges Geotekniske Institutt) er et internasjonalt ledende senter for forskning og rådgivning innen ingeniørrelaterte geofag. Vi tilbyr ekspertise om jord, berg og snø og deres påvirkning på miljøet, konstruksjoner og anlegg, og hvordan jord og berg kan benyttes som byggegrunn og byggemateriale.

Vi arbeider i følgende markeder: Offshore energi – Bygg, anlegg og samferdsel – Naturfare – Miljøteknologi.

NGI er en privat næringsdrivende stiftelse med kontor og laboratorier i Oslo, avdelingskontor i Trondheim og datterselskap i Houston, Texas, USA og i Perth, Western Australia.

www.ngi.no

OSLO
TRONDHEIM
HOUSTON
PERTH

NORWEGIAN GEOTECHNICAL INSTITUTE
NGI.NO

Main office
PO Box 3930 Ullevaal St.
NO-0806 Oslo
Norway

Trondheim office
PB. 5687 Torgarden
NO-7485 Trondheim
Norway

T (+47)22 02 30 00
F (+47)22 23 04 48
NGI@ngi.no

BIC NO. DNBANOKK
IBAN NO26 5096 0501 281
ORGANISATION NO.
958 254 318MVA

ISO 9001/14001
CERTIFIED BY BSI
FS 32989 / EMS 612006